Available online at www.sciencedirect.com

ScienceDirect

Procedia Structural Integrity 44 (2023) 1594–1601

Structural Integrity Procedia

www.elsevier.com/locate/procedia

XIX ANIDIS Conference, Seismic Engineering in Italy

Investigation of a butterfly-arch stress-ribbon pedestrian bridge under ambient excitation: dynamic identification, FE modelling and parametric optimization

Leqia He[a], Chiara Castoro[b]*, Angelo Aloisio[b], Zhiyong Zhang[a], Giuseppe C. Marano[a], Amedeo Gregori[b], Changgen Deng[c] and Bruno Briseghella[a]

[a]*Sustainable and Innovative Bridge Engineering Research Center, College of Civil Engineering, Fuzhou University, China;*
bDepartment of Civil, Construction-Architectural and Environmental Engineering, University of L'Aquila, Italy;
[c]*Department of Structural Engineering, Tongji University, China*

Abstract

The dynamic behavior of a butterfly-arch stress-ribbon pedestrian bridge located in Fuzhou, Fujian, China was investigated under ambient excitation. Highly synchronous tri-axial wireless sensors were used to get an estimate of the model parameters, finding eight stable modes with bending and torsional deformations in the frequency range 3.59–14.92 Hz. Different finite element models of the bridge were developed and a parametric optimization process with a sensitivity-based algorithm was performed to achieve the best model which could be used as baseline for a long-term monitoring of the bridge.

Keywords: Structural Health Monitoring (SHM); Butterfly-arch stress-ribbon pedestrian bridge; operational modal analysis; finite element modelling; sensitivity-based model updating;

1. Introduction

Stress-ribbon structures are considered an elegant and environmental-friendly solution for pedestrian bridges (Strasky, 2005). The simplicity of the structural system consists of a prestressed concrete deck supported by suspension

* Corresponding author.
E-mail address: chiara.castoro@graduate.univaq.it

10.1016/j.prostr.2023.01.204

cables. The suspension cables are embedded in the deck, which follows a catenary arch between the supports. The environmental-friendly characteristic of these structures derives from the economy of the building materials requested for their construction. The first example of stress-ribbon bridge was the Leonel Viera Bridge, completed in 1965, and after this, several similar structures were built worldwide. These structures are characterised by very low natural frequencies, making the deck sensitive to the effect of human-induced vibrations. Therefore, several scholars investigated the dynamic identification and long-term monitoring of these structures (Caetano and Cunha (2004), Hu, Caetano, and Cunha (2013)) finding that these bridges are very prone to exhibit uncomfortable vibrations due to walking excitation. They observed that existing formulations for predicting the maximum acceleration response overestimate the experimental finding. Interestingly, stress-ribbon bridges with a reduced span may exhibit a vibration response lower than expected. Cara, Magdaleno, and Lorenzana (2017); Soria, Dıaz, Garcıa-Palacios, and Iban (2016) also investigated the dynamic response of stress-ribbon structures, but they did not direct on the estimation of the human-induced vibrations. Several passive and active vibration control systems have been developed to investigate vibrations on stress-ribbon bridges (Caetano, Cunha, Magalhaes, & Moutinho (2010) p.1; Setra (2006) Bleicher, Schlaich, Fujino, & Schauer (2011).

The current research focuses on the dynamic assessment and finite element (FE) modelling of a stress-ribbon footbridge located in Fuzhou University, Fuzhou, Fujian, China. In particular, the structure considered in this study is not like conventional stress-ribbon footbridges because it is based on a novel design concept: the combination of a stress-ribbon deck and a butterfly-arch bridge that provides the solution for a self-anchored structural system (Strasky, 2010).

The current case study is the first example of this structural system in China (He et al., 2019) and not many others of this kind are present worldwide. The aim of this study is to investigate the dynamic behavior of the bridge and develop a highly accurate FE model which can serve as baseline for a long-term monitoring of the bridge during its life-cycle (Briseghella et al., 2012; Liu, Zhang, Zordan, & Briseghella, 2016; Zordan, Briseghella, & Liu, 2014). Moreover, the aim is to provide some recommendations for the modelling and analysis of this kind of footbridges.

2. Description of the bridge and dynamic identification

The pedestrian bridge is composed of a stress-ribbon deck and two outward inclined Concrete-Filled Steel Tubular (CFST) arches with interconnecting steel beams (Figure 1). The construction site is on deep soft soils, so the structural solution of a stress-ribbon arch bridge was a perfect choice for its aesthetic values and the self-anchored system, which loads the foundation only in the vertical direction.

Fig. 1. The butterfly-arch stress-ribbon pedestrian bridge in Fuzhou University, Fuzhou, Fujian, China.

The span of the prominent steel tubular arches is 25m with a rise of 5.5 m, see Figures 1 and 2. The dimensions of the cross sections are 42.6 cm-diameter and 1.6 cm-thickness. An outward inclination angle of 30 degrees (counted from the vertical direction) is provided for the prominent arches known as the butterfly arches. There are also secondary steel tubular arches with a smaller cross section 37.7 cm-diameter and 1.6 cm-thickness, for a span of 16.8 m. Welded joints are designed between the main and secondary arches and between the cross beams and secondary arches. The stress-ribbon deck is assembled from precast concrete segments (each one 6m in width, 1.15m in length

and 0.25m in thickness) and is prestressed by two external tendons. The tendons are formed by two bundles of 12xΦ15.2mm mono-strands grouted inside the galvanized steel tubes. The central part of the deck over the river simply rests on the cross beams, while the side parts of the deck hang down freely between the cross beams and the abutments.

Operational modal analysis was performed with a total of 22 nodes that were measured on the bridge deck. In Figure 2 it is represented the setup for the measurement nodes. The acquisition system used was the GMSplus wireless measurement system of the GeoSIG company, sampling at 200 Hz. Two reference sensors and two roving sensors were used for a total of 11 experimental setups. For each setup, the reference sensors were fixed in Nodes 2 and 16. The choice of the reference nodes was derived from a study of the numerical modal characteristics as predicted by a preliminary FE model. The roving sensors, instead, were moved from the right side of the bridge to the left side of the bridge. The roving sensors were placed adjacent to the reference ones at the reference nodes. Each sensor unit was embedded with the tri-axial MEMS accelerometer, which allowed for the synchronous record of the structural vibration responses in all the vertical, transverse, and longitudinal directions. The measurements period was 15 min for each experimental setup. During the testing period, the bridge was under ambient excitation, which included mild winds and low-density pedestrians. In particular, the traffic situations can be classified as ‘individual pedestrians and small groups’ (Feldman, 2008).

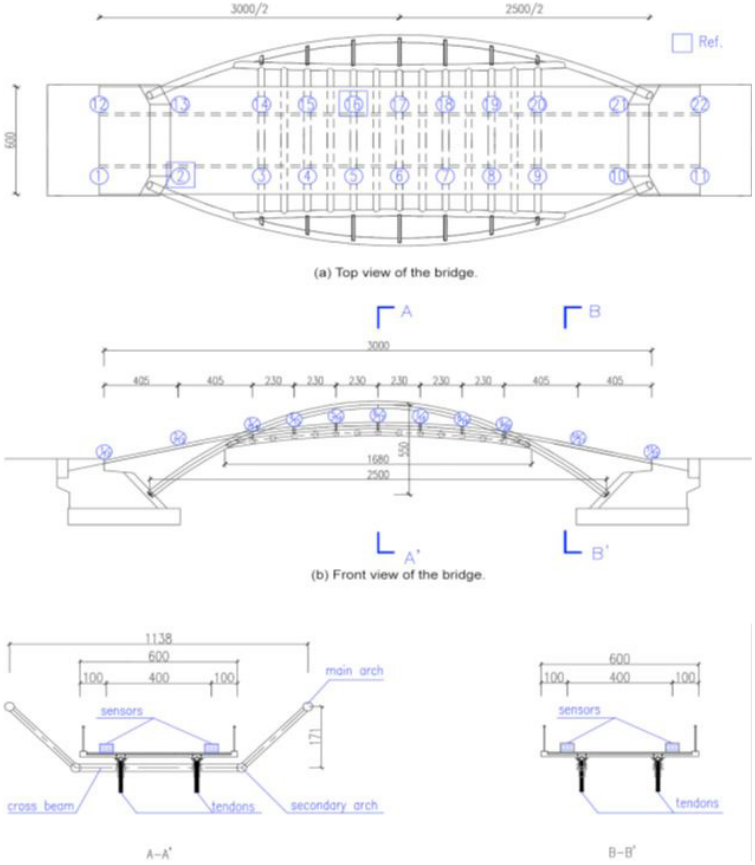

Fig. 2. Deployment of the measurement nodes, labelled from 1 to 22: top view (a), front view (b), sections (c). The reference nodes are Nodes 2 and 16 (units in cm).

Signal processing and system identification were carried out by using the MACEC software (Reynders, Schevenels, & De Roeck, 2011). Modal identification was performed by using the reference-based Stochastic Subspace Identification (SSI) algorithm (Peeters & De Roeck, 1999). Identification results of the OMA are provided in Figures 3 and 4. Eight modes were identified: five vertical bending modes V1, V2, V3, V4, V5 and three torsional modes T1, T2, T3. Most of the identified experimental modes are symmetric and anti-symmetric, since the structure is symmetric.

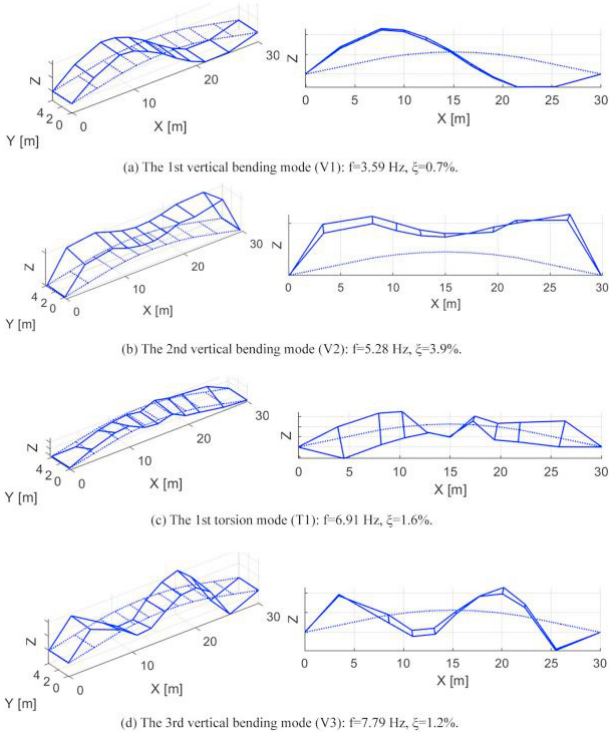

(a) The 1st vertical bending mode (V1): f=3.59 Hz, ξ=0.7%.

(b) The 2nd vertical bending mode (V2): f=5.28 Hz, ξ=3.9%.

(c) The 1st torsion mode (T1): f=6.91 Hz, ξ=1.6%.

(d) The 3rd vertical bending mode (V3): f=7.79 Hz, ξ=1.2%.

Fig. 3. The first four experimental mode shapes

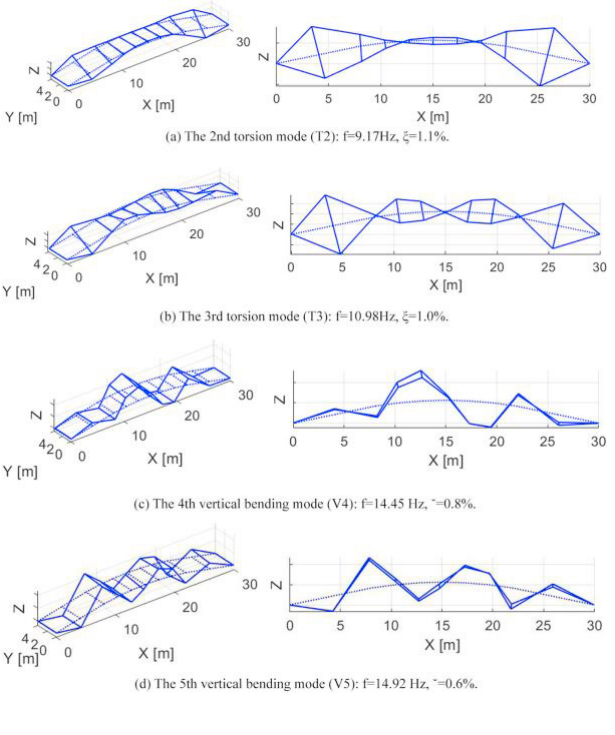

(a) The 2nd torsion mode (T2): f=9.17Hz, ξ=1.1%.

(b) The 3rd torsion mode (T3): f=10.98Hz, ξ=1.0%.

(c) The 4th vertical bending mode (V4): f=14.45 Hz, ˜=0.8%.

(d) The 5th vertical bending mode (V5): f=14.92 Hz, ˜=0.6%.

Fig. 4. The second four experimental mode shapes.

Losses of symmetry are found for the last two vertical bending modes, V4 and V5, and it might be due to the uneven distribution of the stiffness or mass, such as those related to the uncertainty of the stress ribbon deck. Moreover, experimental errors and construction uncertainties might also have contributed to some irregularity in the mode shapes. The fundamental frequency was found at 3.59Hz in vertical bending. No lateral bending mode was found. Generally, the usual fundamental frequencies of this kind of structures are in the range (2 - 4Hz) even though Zivanovic, Pavic, and Reynolds (2005) state that the range could be different, depending on the rigid surface on which the measurement are done. Modal Assurance Criterion (MAC) values were calculated between the experimental modes. They were found to be no higher than 0.1 for the first six modes. This suggests that the identified modes were almost linearly independent.

3. Finite element modelling, implementation, and parametric updating

During the design stage, a preliminary FE model was developed in SAP2000, see Figure 5(a). The arches, cross beams and prestressed tendons were modelled as 3D-beam elements. The precast concrete slabs were also modelled by longitudinal beams and rigid links were added between the slabs and the tendons to represent the mutual offsets in the real structure. Fixed boundaries on both the main arches springs and the stress ribbons anchors/tendons were adopted. The following first-attempt material properties have been considered in the model: equivalent elastic modulus of concrete E_c = 36.750 MPa, density of concrete ρ_c = 2500 kg/m^3, equivalent elastic modulus of steel E_s = 210.000 MPa, density of steel ρ_s = 7850 kg/m^3. Table 1 presents the results of this first FE model. $\Delta f = (f_{FEM} - f_{EXP}) / f_{EXP}$ defines the relative differences between the experimental natural frequencies and the numerical ones. The Modal Assurance Criterion (MAC) is used to express the correspondence between the numerical and experimental modal parameters. It can be noted that the MAC values are higher than 0.6 overall. In particular, the torsion modes T1 and T2 present MAC values equal to 0.6 and present higher relative differences in frequency compared to the vertical bending modes. Moreover, the third torsional mode T3, the vertical mode V4 and the vertical mode V5 are not predicted by this model. It was concluded that the model did not reflect the real structure's behavior as a self-balanced system and a second FE model, depicted in Figure 5(b), was developed. In this second model, fixed constraints were removed, and spring elements were introduced in the three-axial directions to represent the soil effects. Additionally, rigid link elements were added between the ends of the deck and the arches springs to simulate the abutments. Table 2 reports the natural frequencies of this model compared to the experimental modes. Compared to the first model, this second model considers the actual behavior of the abutments. Despite the lower differences in frequency compared to those observed in the first model, in this second model the torsional modes T2 and T3, together with the vertical modes V4 and V5 are not found. It is possible that the discrepancies originate from adopting beam-like elements. Since the bridge deck was simplified into longitudinal beam elements, the torsional behavior of the structure cannot be accurately predicted (Aloisio, Alaggio, & Fragiacomo, 2020a, 2020b).

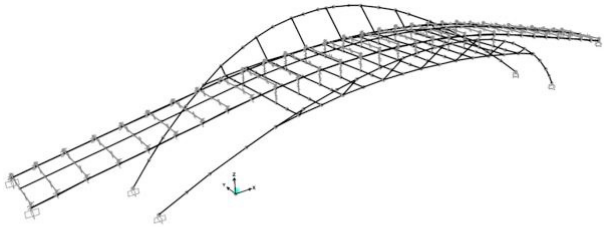

(a) 1st FE model with fixed boundaries and without the abutments.

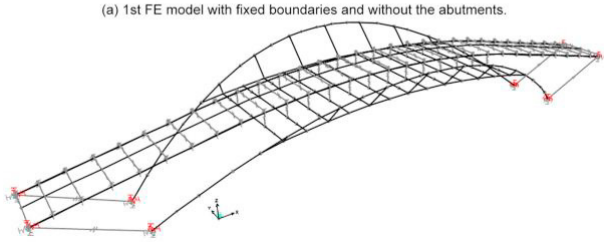

(b) 2nd FE model with soil springs and rigid elements for the abutments.

Fig. 5. View of the first and second FE models with only 3D-beam elements.

Table 1. Comparison between experimental and numerical modal parameters and the first FE model.

Nr. of modes	Type	f_{exp}(Hz)	f_{fem1}(Hz)	Δf_1(%)	MAC_1
1	V1	3.59	4.08	13.8	0.98
2	V2	5.28	7.35	39.2	0.81
3	T1	6.91	10.71	55.0	0.58
4	V3	7.79	9.74	25.0	0.66
5	T2	9.17	16.24	77.1	0.62

Table 2. Comparison between experimental and numerical modal parameters and the second FE model.

Nr. of modes	Type	f_{exp}(Hz)	f_{fem2}(Hz)	Δf_2(%)	MAC_2
1	V1	3.59	3.71	3.3	0.99
2	V2	5.28	4.51	–14.5	0.81
3	T1	6.91	8.21	18.8	0.61
4	V3	7.79	11.28	44.8	0.94

For these reasons, a third FE model was implemented, shown in Figure 6. In this model, shell elements, 6m wide, 1.15m long and 0.25m thick, replaced the 3D-beam elements as better representatives of the concrete deck. A sensitivity analysis confirmed that a mesh size of 0.5m x 0.29m is the optimum balance between the computational costs and the accuracy of the results. Moreover, the 3Dbeams of the CFST arches, cross beams, and hangers, were modelled more accurately according to their actual shape. The materials properties set for the third model are: equivalent elastic modulus of the concrete deck E_c = 40.000 MPa, density of the concrete deck ρ_c = 2600 kg/m^3, equivalent elastic modulus of the filling concrete inside the tubular steel E_{cf} = 42.000 MPa, density of the filling concrete ρ_{cf} = 2400 kg/m^3, equivalent elastic modulus of steel E_s = 210.000 MPa, density of steel ρ_s = 7850 kg/m^3, equivalent elastic modulus of tendons E_t = 206.000 MPa, density of tendons ρ_t = 7850 kg/m^3. Compared to the previous models, the third model determines a tangible improvement in frequency agreement (Table 3).

Table 3. Comparison of the experimental modal data with the results of the third FE model and the relative updated model.

Nr. of modes	Type	f_{exp}(Hz)	f_{fem3}(Hz)	Δf_3(%)	MAC_3	f_{fem3ud}(Hz)	Δf_{3ud}(%)	MAC_{3ud}
1	V1	3.59	3.07	–14.25	0.97	3.38	–5.85	0.99
2	V2	5.28	4.73	–10.35	0.94	5.01	–5.02	0.97
3	T1	6.91	6.15	–11.01	0.79	6.71	–2.83	0.89
4	V3	7.79	8.11	4.14	0.86	8.14	4.53	0.87
5	T2	9.17	9.02	–1.68	0.83	9.51	3.74	0.89
6	T3	10.98	11.18	1.81	0.71	10.94	–0.41	0.82

The relative frequency differences for the torsional modes T1 and T2 reduced from 55.0% to - 11.01% and from 77.1% to -1.68%, respectively. Interestingly, the third torsional mode T3 was found with a 1.81% relative difference. The vertical bending modes V4 and V5 were instead not found. In this regard, it should be noted that, for these two vertical modes, the MAC values calculated for the experimental modal parameters were quite low, 0.4 and 0.5, respectively. To minimize the differences between the numerical and experimental results, a sensitivity-based model updating (Fa et al., 2016; Mottershead, Link, & Friswell, 2011) of the third FE model was performed. In detail, a nonlinear least-squares problem was solved minimizing the residuals between the experimental and numerical modal data. The sensitivity-based model updating was implemented into an interactive procedure based on MATLAB by applying the embedded Levenberg–Marquardt algorithm (Moré, 1978), and SAP2000. The stiffness of the springs, elastic modulus of the concrete deck E_c and the elastic modulus of the tendons E_t were chosen as updating parameters. The choice was made based on a sensitivity analysis which included also E_{cf} and E_s. Table 3 reports the modal data of the updated third model. The updated model shows reduced relative differences of frequency for a maximum of -5.85%. MAC values result higher than 0.82.

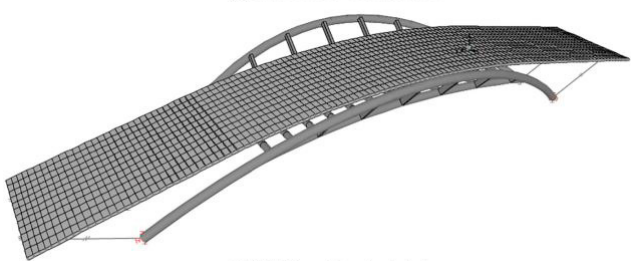

Fig. 6. View of the third FE model with shell elements for the concrete deck.

These results confirm that the updated third model provides more accurate and reliable predictions of the current modal characteristics of the structure. The values of the parameters obtained after the updating are E_c = 57,600 MPa and E_t = 225,100 MPa, which are realistic values for the representing parameters, considering a high strength concrete used for the precast panels which may include also reinforcing bars. The improved modelling and parametric updating minimized the differences between the numerical and experimental modal parameters, endorsing the accuracy of the obtained FE model. At this purpose, a remark should be done: since footbridges are structures having a predominant dimension, simple FE models using only beam elements are generally employed with good results (Pimentel, 1997) to simulate their dynamic behavior. However, it is observed sometimes that simplified models fail in simulating complex mechanisms, and this is the case. Of course, improved FE models can be characterized by several levels of complexity and computational cost (Gregori, Castoro, Mercuri, & Angiolilli, 2021; Mercuri, Pathirage, Gregori, & Cusatis, 2020) and the choice of the most appropriate modelling approach depends on the desired levels of accuracy and simplicity at the same time. In this case, an accurate modelling resolution is required to simulate adequately the behavior of the structure under ambient vibration.

4. Conclusions

The article presents the outcomes of dynamic identification and finite element modelling of a butterfly-arch stress-ribbon pedestrian bridge located in Fuzhou, Fujian, China. Operational Modal Analysis returned the estimate of eight modes in the frequency range 3.59–14.92 Hz. FE modelling implementations were developed to assess the optimum modelling choices for achieving a satisfactory agreement between the model prediction and the experimental data. The structure is not like conventional stress-ribbon footbridges, since it is based on a novel design concept which is the combination of a stress-ribbon deck and a butterfly-arch bridge that provides the solution for a self-anchored structural system. An accurate modelling resolution was required to simulate adequately the behavior of this kind of structure under ambient excitation. Three different FE models with increasing accuracy were developed. The discrepancies originated from adopting beam-like elements were overcome using shell elements to better represent the behavior of the concrete deck and with the parametric optimization procedure a satisfactory agreement between the model prediction and the experimental data was achieved.

The study demonstrates the importance of the modelling strategy in simulating the dynamic behavior of complex footbridges, as the one considered in this research, in comparison to traditional bridges which can be modelled following simplified modelling procedures. Finally, the developed FE model could be used as baseline for long-term monitoring of the bridge and could represent a guide to practitioners and scholars for the modelling and analysis of this kind of structures.

References

Aloisio, A., Alaggio, R., & Fragiacomo, M. (2020a). Dynamic identification and model updating of full-scale concrete box girders based on the experimental torsional response. Construction and Building Materials, 264, 120146. doi:10.1016/j.conbuildmat.2020.120146

Aloisio, A., Alaggio, R., & Fragiacomo, M. (2020b). Time-domain identification of the elastic modulus of simply supported box girders under moving loads: Method and full-scale validation. Engineering Structures, 215, 110619. doi:10.1016/j.engstruct.2020.110619

Bleicher, A., Schlaich, M., Fujino, Y., & Schauer, T. (2011). Model-based design and experimental validation of active vibration control for a stress ribbon bridge using pneumatic muscle actuators. Engineering Structures, 33(8), 2237–2247. doi:10.1016/j.engstruct.2011.02.035

Briseghella, B., Chen, A., Li, X., Zordan, T., Lan, C., & Mazzarolo, E. (2012). Analysis on applicability of health monitoring techniques on a curved cable stayed bridge. Bridge Maintenance, Safety, Management, Resilience and Sustainability–Proceedings of the Sixth International Conference on Bridge Maintenance, Safety and Management (pp. 2617–2624).

Caetano, E., & Cunha, A. (2004). Experimental and numerical assessment of the dynamic behaviour of a stress-ribbon footbridge. Structural Concrete, 5(1), 29–38. doi:10.1680/stco.2004.5.1.29

Caetano, E., Cunha, _A., Magalh~aes, F., & Moutinho, C. (2010). Studies for controlling human-induced vibration of the pedro e in^es footbridge, Portugal. Part 1: Assessment of dynamic behaviour. Engineering Structures, 32(4), 1069–1081. doi:10.1016/j.engstruct.2009.12.034

Cara, J., Magdaleno, A., & Lorenzana, A. (2017). Input/output versus output only modal ana-lysis of a stress-ribbon footbridge. IOMAC 2017–7th International Operational Modal Analysis Conference.

Fa, G., He, L., Fenu, L., Mazzarolo, E., Briseghella, B., & Zordan, T. (2016). Comparison of direct and iterative methods for model updating of a curved cable-stayed bridge using experimental modal data. Proceedings of the IABSE Conference (pp. 8–11), Guangzhou, China. doi:10.2749/222137816819258816

Feldman, M. (2008). Hivoss—human-induced vibrations of steel structures. Luxembourg: Office for Official Publications of the European Communities.

Gregori, A., Castoro, C., Mercuri, M., & Angiolilli, M. (2021). Numerical modelling of the mechanical behaviour of rubbercrete. Computers & Structures, 242(106393), 106393. doi: 10.1016/j.compstruc.2020.106393

He, L., Zhang, Z., Marano, G. C., Briseghella, B., Xue, J., & Ni, Z. (2019). Dynamic characterization of a stress ribbon and butterfly arch pedestrian bridge using wireless measurements. Proceedings of ARCH 2019: 9th International Conference on Arch Bridges (Vol. 11, pp. 395). Springer Nature.

Hu, W.-H., Caetano, E., & Cunha, _A. (2013). Structural health monitoring of a stress-ribbon footbridge. Engineering Structures, 57, 578–593. doi:10.1016/j.engstruct.2012.06.051

Liu, T., Zhang, Q., Zordan, T., & Briseghella, B. (2016). Finite element model updating of canonica bridge using experimental modal data and genetic algorithm. Structural Engineering International, 26(1), 27–36. doi:10.2749/101686616X14480232444405

Mercuri, M., Pathirage, M., Gregori, A., & Cusatis, G. (2020). Computational modeling of the out-of-plane behavior of unreinforced irregular masonry. Engineering Structures, 223(111181), 111181. doi:10.1016/j.engstruct.2020.111181

More, J. J. (1978). The levenberg-marquardt algorithm: Implementation and theory. In Numerical analysis (pp. 105–116). Springer.

Mottershead, J. E., Link, M., & Friswell, M. I. (2011). The sensitivity method in finite element model updating: A tutorial. Mechanical Systems and Signal Processing, 25(7), 2275–2296. doi:10.1016/j. ymssp.2010.10.012

Peeters, B., & De Roeck, G. (1999). Reference-based stochastic subspace identification for output-only modal analysis. Mechanical Systems and Signal Processing, 13(6), 855–878. doi:10.1006/mssp. 1999.1249

Pimentel, R. (1997). Vibrational performance of pedestrian bridges due to human-induced loads (Ph.D. thesis). Univeristy of Sheffield, Sheffield, UK.

Reynders, E., Schevenels, M., & De Roeck, G. (2011). Macec 3.2: A MATLAB toolbox for experimental and operational modal analysisuser's manual. Leuven: Katholieke Universiteit.

Setra, F. (2006). Assessment of vibrational behaviour of footbridges under pedestrian loading. Technical guide SETRA. Paris, France.

Soria, J. M., Dıaz, I. M., Garcıa-Palacios, J. H., & Iban, N. (2016). Vibration monitoring of a steel-plated stress-ribbon footbridge: Uncertainties in the modal estimation. Journal of Bridge Engineering, 21(8), C5015002. doi:10.1061/(ASCE)BE.1943-5592.0000830

Strasky, J. (2005). Stress ribbon and cable-supported pedestrian bridges. Thomas Telford.

Strasky, J. (2010). Stress-ribbon pedestrian bridges supported by arches. Concrete International, 32(5), 28–33.

Zivanovic, S., Pavic, A., & Reynolds, P. (2005). Vibration serviceability of footbridges under human-induced excitation: A literature review. Journal of Sound and Vibration, 279(1–2), 1–74. doi:10.1016/j.jsv. 2004.01.019

Zordan, T., Briseghella, B., & Liu, T. (2014). Finite element model updating of a tied-arch bridge using douglas-reid method and rosenbrock optimization algorithm. Journal of Traffic and Transportation Engineering (English Edition), 1(4), 280–292. doi:10.1016/S2095-7564(15)30273-7